清華大學地球系统科学系
Department of Earth System Science, Tsinghua University

EGU General Assembly 2024

iPyCLES in PICO

Large-Eddy Simulations of the Isotopic Signatures of Arctic Mixed-Phase Stratocumulus Clouds Under Different Surface and Atmospheric Conditions

Reportor: **Hu Zizhan**, Jonathon Wright

2024.4.16, Vienna, EGU24, AS 2.5

Hu, Z., Peng, Y., Zhu, M., and Wright, J. S.: iPyCLES v1.0: A New Isotope-Enabled Large-Eddy Simulator for Mixed-Phase Clouds, EGUsphere [preprint], https://doi.org/10.5194/egusphere-2024-828, 2024.

iPyCLES Source Code on Github

iPyCLES Paper Preprinted in GMD

A New Isotope Enabled LES: iPyCLES

Iso-GCM/RCM

- ICON-ART-Iso
- NCAR CAM2
- GISS II
- REMOiso

- Current modeling of isotopes in **large-scale models** **can't represent strong isotopic fractionation** during unresolved (subgrid) processes
- To address this issue we developed a full-featured iso-enabled Large Eddy Simulation Model (LES): **iPyCLES**

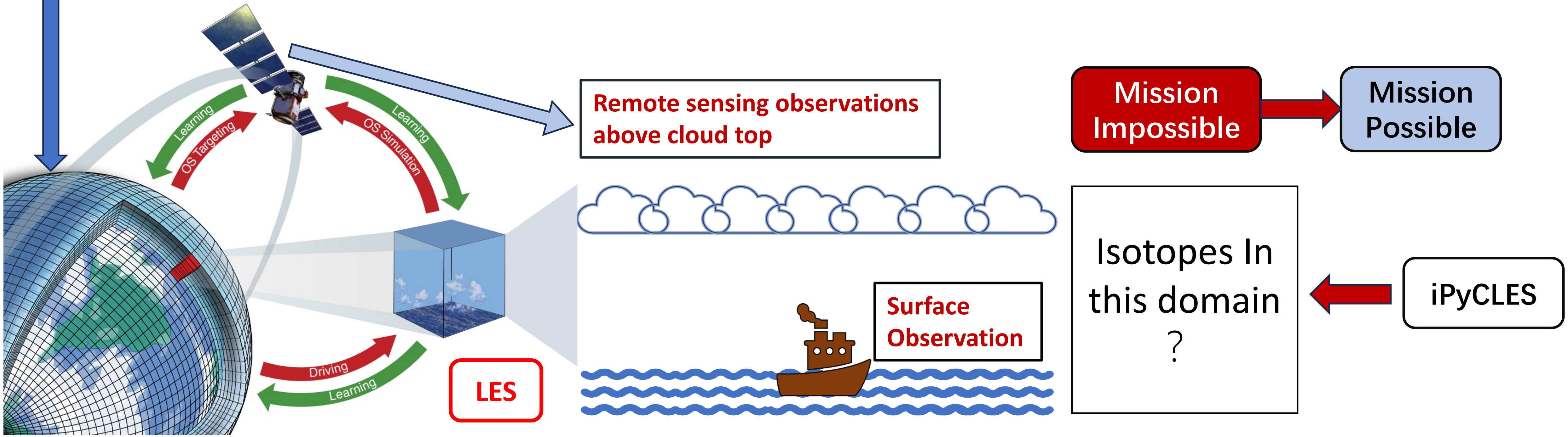

Experiments Under different Atmosphere and Surface Condtions

Motivated by **MOSAiC observation**：
Can iPyCLES help to identify **isotopic signals of atmospheric environmental variations affecting Arctic mixed-phase clouds**?
Four experiments are conducted based on the ISDAC observation campaign.

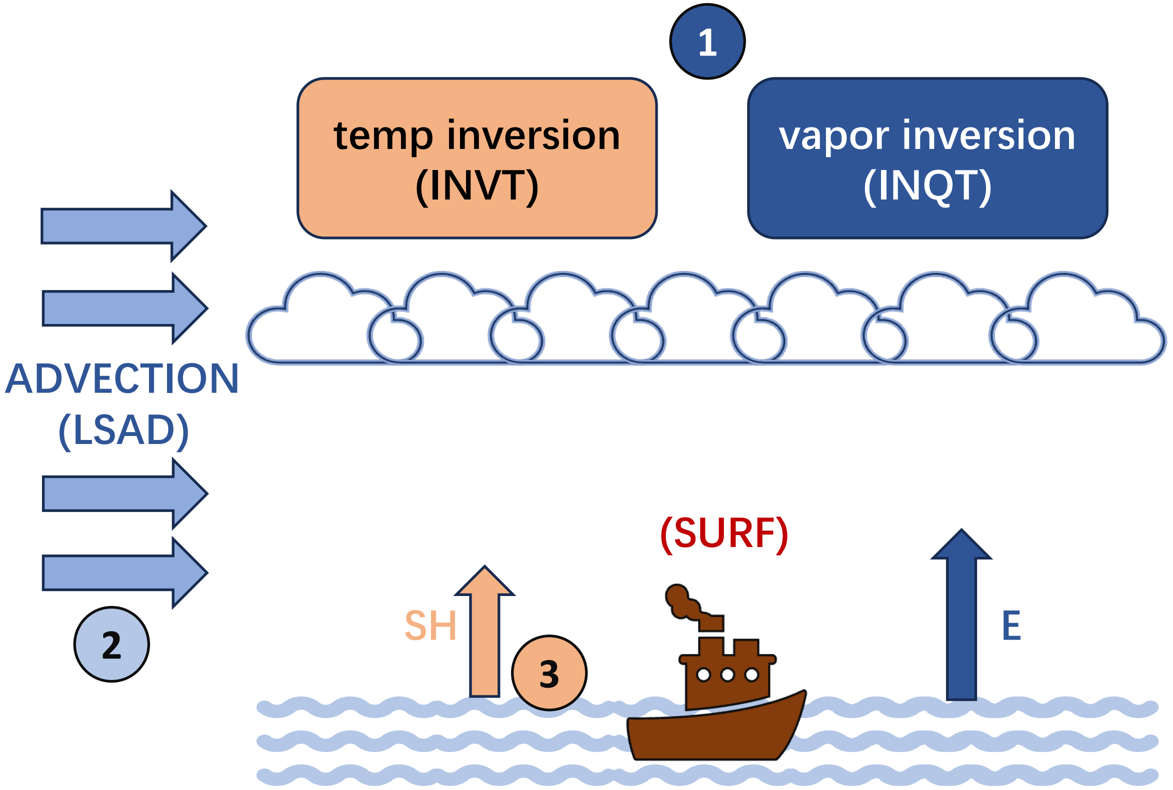

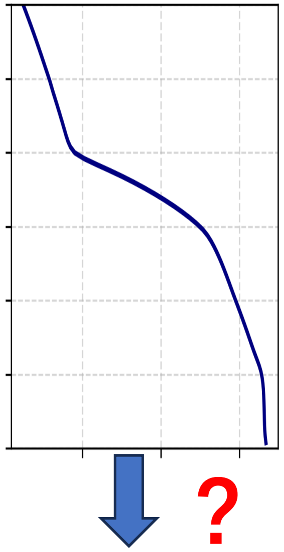

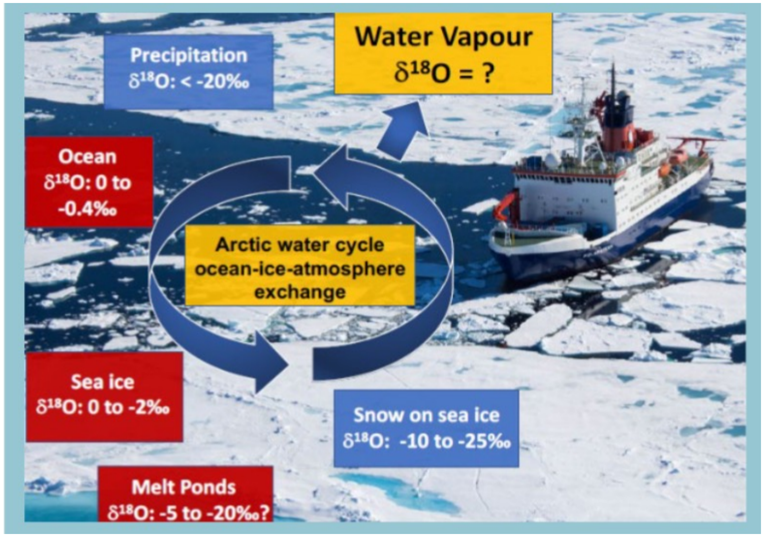

MOSAiC Observation

Conclusion

- This study demonstrates **the potential of iPyCLES** for atmospheric water **isotopes to provide new observational constraints** on interactions between Arctic mixed-phase clouds and their environment.
- Isotopic composition in water species, like **vapor and snow, which are readily observable with current technologies, shows sensitivity** to the different environmental settings.

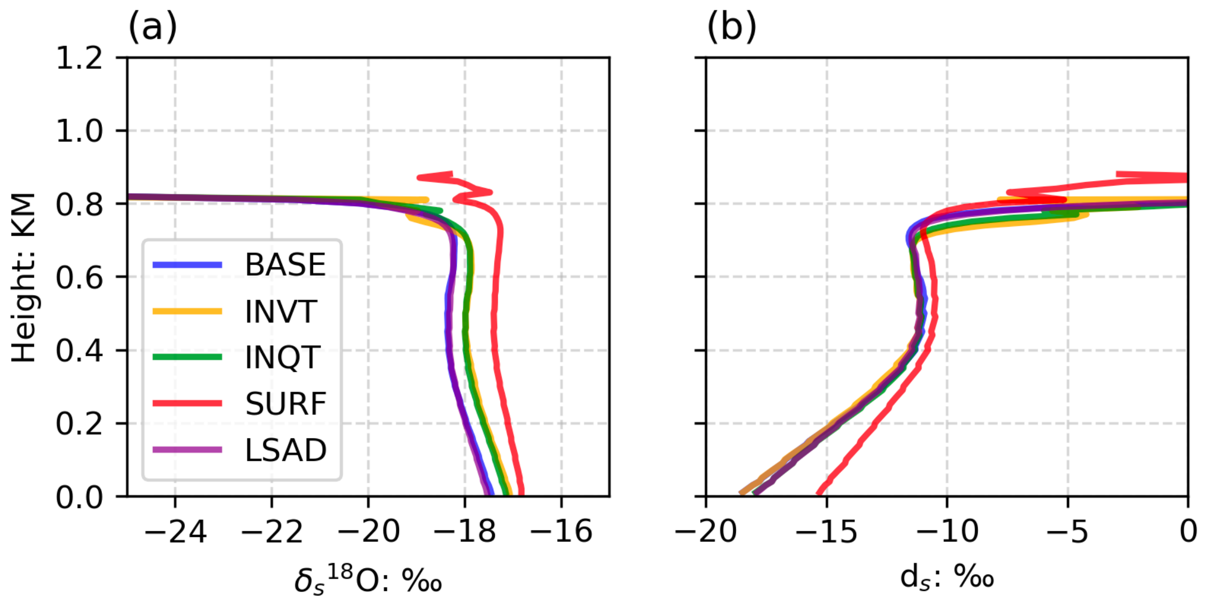

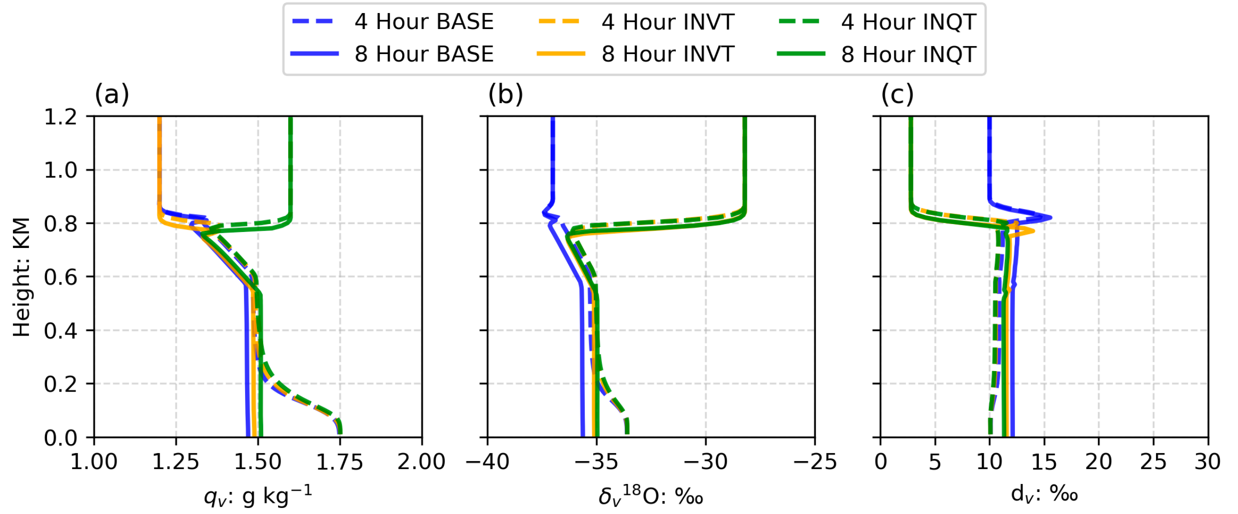

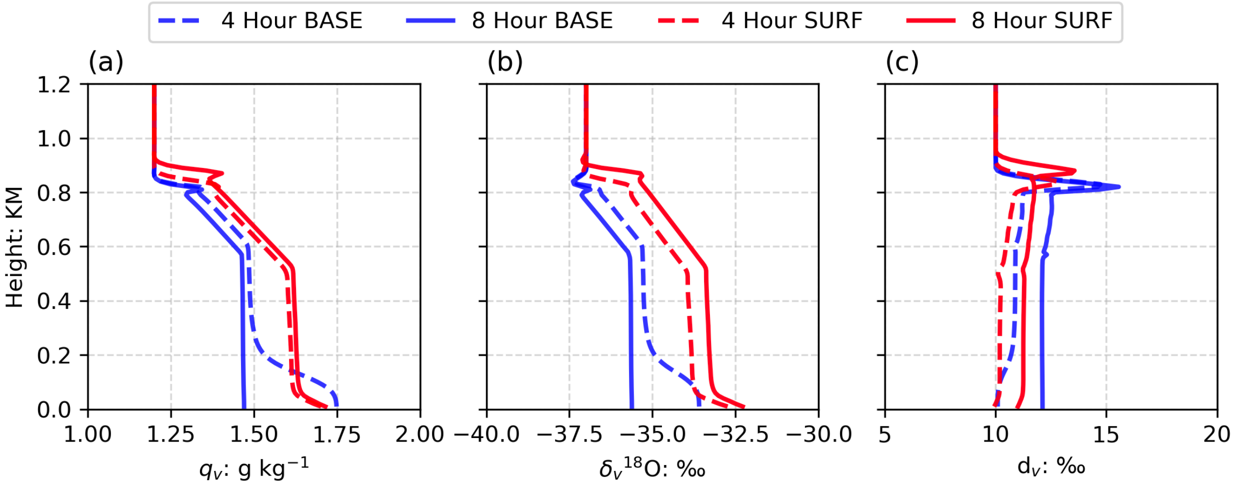

Supplementary Material： iPyCLES

iPyCLES Structure

Passive Tracer

Uniaxially take dynamics and thermo

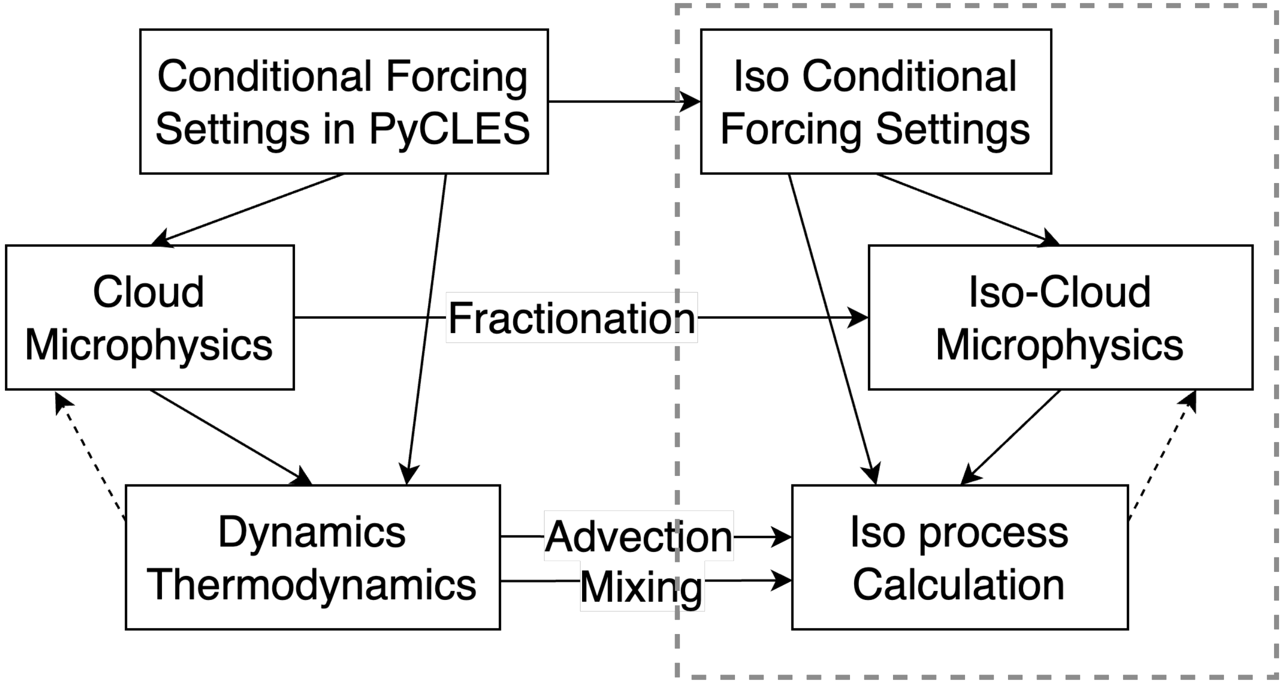

Balance Equation

SGS turbulance

$$\frac{\partial q_{iso}}{\partial t} + \frac{1}{\rho_0}\frac{\partial(\rho_0 u_i q_{iso})}{\partial x_i} = -\frac{1}{\rho_0}\frac{\partial(\rho_0 \gamma_{q_{iso},i})}{\partial x_i} + \dot{\Phi}_{iso}$$

Advection

$$\left.\frac{\partial q_{iso}}{\partial t}\right|_{\text{Surface Flux}} + \left.\frac{\partial q_{iso}}{\partial t}\right|_{\text{Boundry Forcing}} + \left.\frac{\partial q_{iso}}{\partial t}\right|_{\text{Cloud Microphysics}}$$

Supplementary Material： iPyCLES and Microphysics

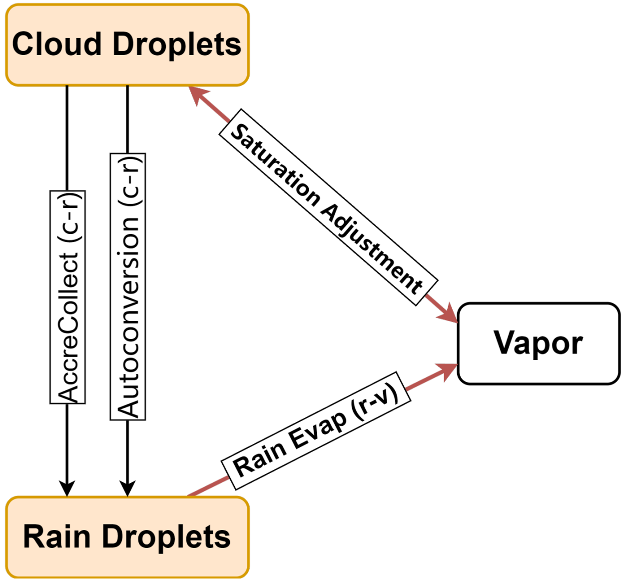

SBWarm

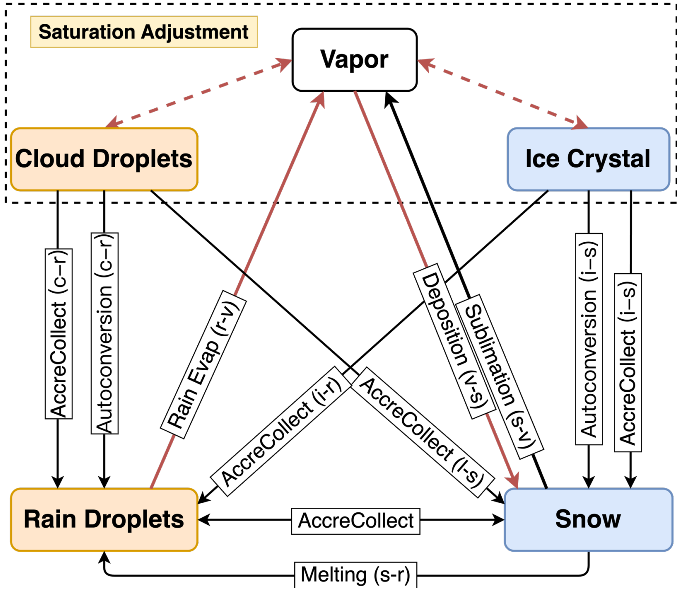

Arctic 1M

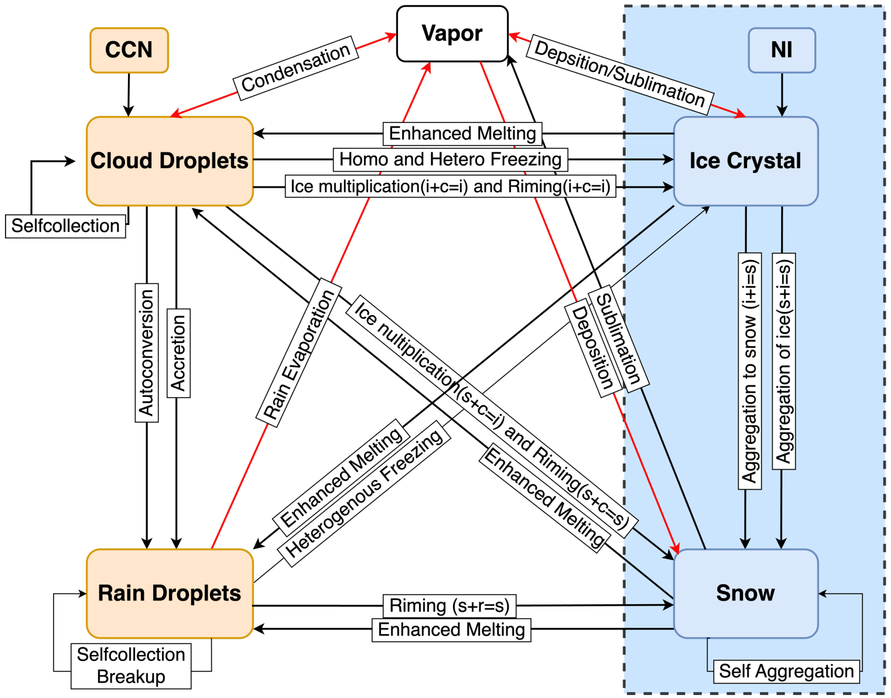

SB Ice 2M

Supplementary Material： iPyCLES Development

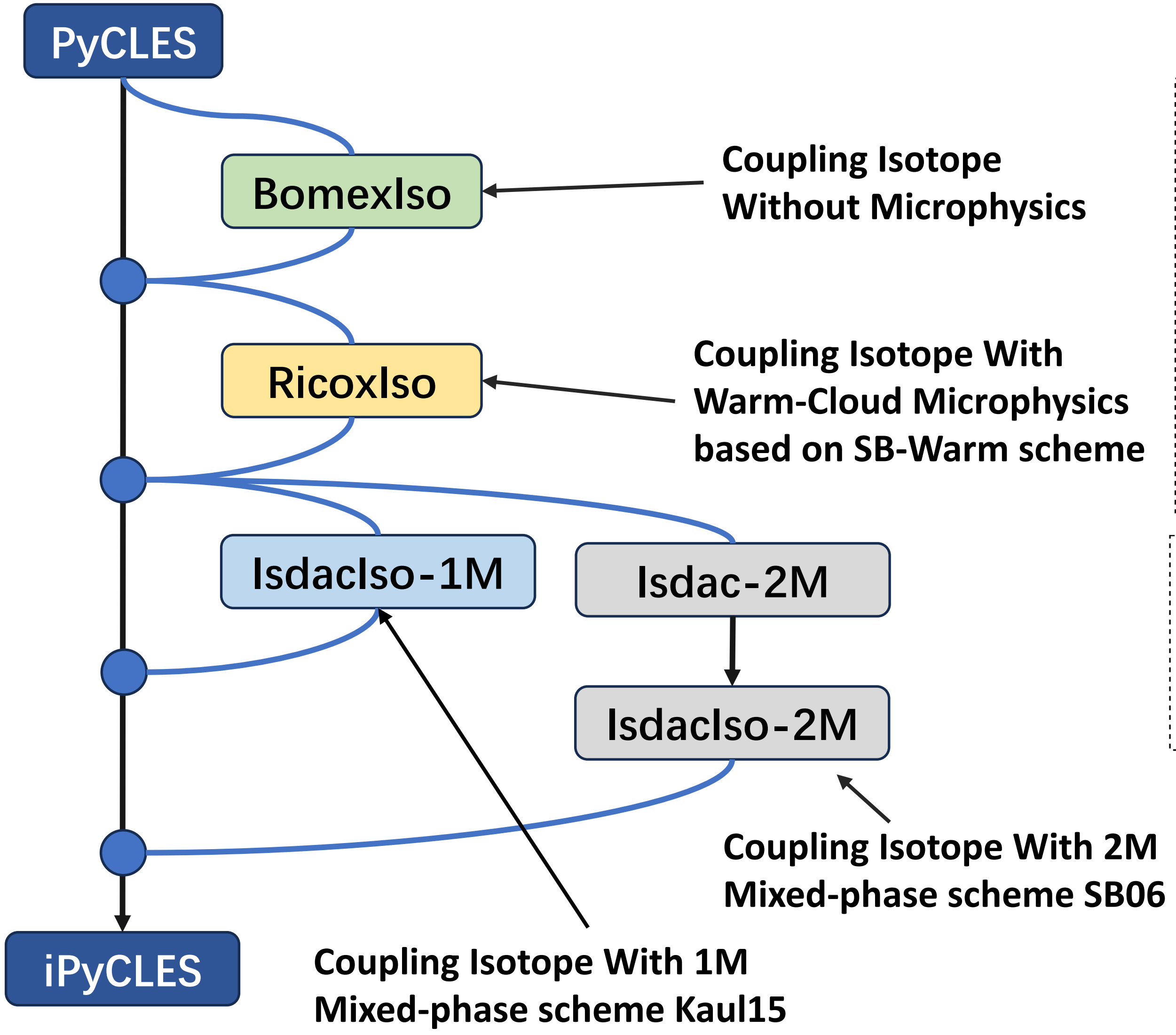

q_t Isotope Default Initialization

$\delta^{18}O = 8.99\ln(q_v/0.622) - 42.9 \quad \delta D = \delta^{18}O \times 8 + 10‰$

q_t^{iso} tendency source

C-G Model Surface Flux Isotope Source Only Apply to q_t and q_t^{iso}

$$R_{eavp} = \frac{\alpha_{eq}\alpha_k R_L}{(1-RH) + \alpha_k RH}$$

Forcing Isotope Source Only Apply to q_t and q_t^{iso}

$$R_{q_t} = \frac{q_t^{iso}}{q_t}$$

Water phase balance
(if q_l and q_i are diagnosed)

$$q_t^{iso} = q_v^{iso} + q_l^{iso} + q_i^{iso}$$

Liquid-vapor is assumed as equilibrium fractionation

$$q_v^{iso} = \frac{q_t^{iso}}{1 + (q_l/q_v) * \alpha_{eq}}$$

Rain Evaporation

$$\frac{\partial q_r^{iso}}{dt} = -4\pi a f' D_v' \left[\frac{R_{rain}}{\alpha} \times \left(\frac{1+b_l S_l}{1+b_l}\right) - R_{vapor} \times S_l\right] \rho_v^* [T(\infty)] \qquad b_l = D_v \rho_v^* \frac{L_c}{kT}\left(\frac{L_c}{R_v T} - 1\right)$$

$$\alpha_{eq}(^{18}O) = \exp(\frac{1137}{T^2} - \frac{0.4156}{T} - 2.0667 \times 10^{-3})$$

$$\alpha_{eq}(HDO) = \exp(\frac{24844}{T^2} - \frac{76.248}{T} - 52.612 \times 10^{-3})$$

Non-Fractional $\frac{\partial q^{iso}}{\partial t} = R_{i,r,s}\frac{\partial q}{\partial t}$

Kaul 15 1M Schem

Rain Autoconversion: Gilmore and Straka 2008

$$\frac{\partial q_r}{\partial t}_{\mathrm{AUT}} = \max(\hat{L}_2', 0) \times \max(\hat{T}_{2inv}, 0)/\rho$$

Snow Autoconversion

$$\frac{\partial q_s}{\partial t}_{aut} = \frac{4\pi}{\rho}(S_i - 1)G_i(T)N_{0,i}\exp(-\lambda_i D_i)\left(\frac{D_b^2}{b_i} + \frac{1+\lambda_i D_b}{\lambda_i^2}\right)$$

All accretion

$$\frac{\partial q_r}{\partial t} = S_r + S_{r-l} + S_{r-i} \qquad \frac{\partial q_l}{\partial t} = -S_{r-l} - S_{rime_{sl}}$$

$$\frac{\partial q_s}{\partial t} = S_s + S_{s-l} + S_{s-i} \qquad \frac{\partial q_i}{\partial t} = -S_{r-i} - S_{s-i}$$

Rain Evaportaion

$$\frac{\partial q_r}{\partial t}_{\mathrm{EVP}} = 2\pi(S_l - 1)\left[0.78 + 0.27\mathrm{Re}_r^{1/2}\right]G_l(T)N_{0,r}\lambda_r^{-2}$$

Snow Dep/Sub

$$\frac{\partial q_s}{\partial t}_{\mathrm{D/S}} = \frac{4}{3}\pi(S_i - 1)\left[0.65 + 0.39\mathrm{Re}_s^{1/2}\right]G_i(T)N_{0,s}\lambda_s^{-2}$$

Snow Melting

$$\frac{\partial q_s}{\partial t}_{\mathrm{MELT}} = -2\pi K_a L_f^{-1}(T - 273.16)[0.65 + 0.39Re_s^{1/2}]\lambda_s^{-2}$$

Ice-vapor is very strong kinetic fractionation

$$\frac{\partial q_i^{iso}}{\partial t} = \alpha_s \alpha_k R_{\mathrm{vapor}} \frac{\partial q_i}{\partial t}$$

$$\alpha_s(^{18}O) = \exp(\frac{11.839}{T} - 2.8224 \times 10^{-2})$$

$$\alpha_s(HDO) = \exp(\frac{16289}{T^2} - 9.45 \times 10^{-2})$$

$$\alpha_k = \frac{(1+b_s)S_s}{\alpha_s \frac{fD_v}{f'D_v'}(S_s - 1)(1-\beta_s) + [1 + b_s S_s + \beta_s(S_s - 1)]}$$

SB06 2M Scheme and Isotope coupling

Cloud Act/Cond $\frac{\partial n_l}{\partial t}_{cat} = C_{ccn}\kappa S^{\kappa-1}\frac{\partial S}{\partial t}w \qquad \frac{\partial q_l}{\partial t}_{act} = x_c \frac{\partial n_l}{\partial t}_{act}$

Ice Nuc/Freez $\frac{\partial n_i}{\partial t}_{nuc} = \frac{n_{IN}(S_i, T) - n_i}{\Delta t} \qquad \frac{\partial q_i}{\partial t}_{nuc} = x_{i,nuc}\frac{\partial n_i}{\partial t}_{nuc}$

Ice/Snow Dep&Sub $\frac{\partial q_{s,i}}{\partial t}_{dep} = \frac{4\pi}{c_i}G_{iv}(T,p)D_i(\bar{x})\bar{F}_{v,1}S_i \qquad G_{iv}(T,p) = \left[\frac{R_v T}{p_{iv}(T)D_v} + \frac{L_{iv}}{K_T T}\left(\frac{L_{iv}}{R_v T} - 1\right)\right]^{-1}$

Ice/Snow Coll

$$\frac{\partial q_{i,s}}{\partial t}_{coll,ab} = \frac{\pi}{4}\bar{E}_{ab}N_a L_b\left[\delta_a^0 D_a^2(\bar{x}_a) + \delta_{ab}^1 D_b(\bar{x}_b)D_a(\bar{x}_a) + \delta_b^1 D_b^2(\bar{x}_b)\right] \times \left[\vartheta_a^0 v_a^2(\bar{x}_a) - \vartheta_{ab}^1 v_b(\bar{x}_b)v_a(\bar{x}_a) + \vartheta_b^1 v_b^2(\bar{x}_b) + \sigma_a + \sigma_b\right]^{\frac{1}{2}}$$

$$\frac{\partial n_{i,s}}{\partial t}_{coll,ab} = -\frac{\pi}{4}\bar{E}_{ab}N_a N_b\left[\delta_a^0 D_a^2(\bar{x}_a) + \delta_{ab}^0 D_b(\bar{x}_b)D_a(\bar{x}_a) + \delta_b^0 D_b^2(\bar{x}_b)\right] \times \left[\vartheta_a^0 v_a^2(\bar{x}_a) - \vartheta_{ab}^0 v_b(\bar{x}_b)v_a(\bar{x}_a) + \vartheta_b^0 v_b^2(\bar{x}_b) + \sigma_a + \sigma_b\right]^{\frac{1}{2}}$$

Snow Melting $\left.\frac{\partial M_i^n}{\partial t}\right|_{\mathrm{melt}} = -\frac{2\pi}{L_{il}}\left[\frac{K_T D_T}{D_v}(T - T_3) + \frac{D_v L_{iv}}{R_v}\left(\frac{p_v}{T} - \frac{p_{lv}(T_3)}{T_3}\right)\right]$

Ice/Snow Dep

$$\frac{\partial q_{i,s}^{iso}}{\partial t} = \alpha_s \alpha_k R_{\mathrm{vapor}}\frac{\partial q_{i,s}}{\partial t} \qquad \alpha_k = \frac{(1+b_s)S_s}{\alpha_s \frac{fD_v}{f'D_v'}(S_s - 1)(1-\beta_s) + [1 + b_s S_s + \beta_s(S_s - 1)]}$$

Supplementary Material：iPyCLES in BOMEX case

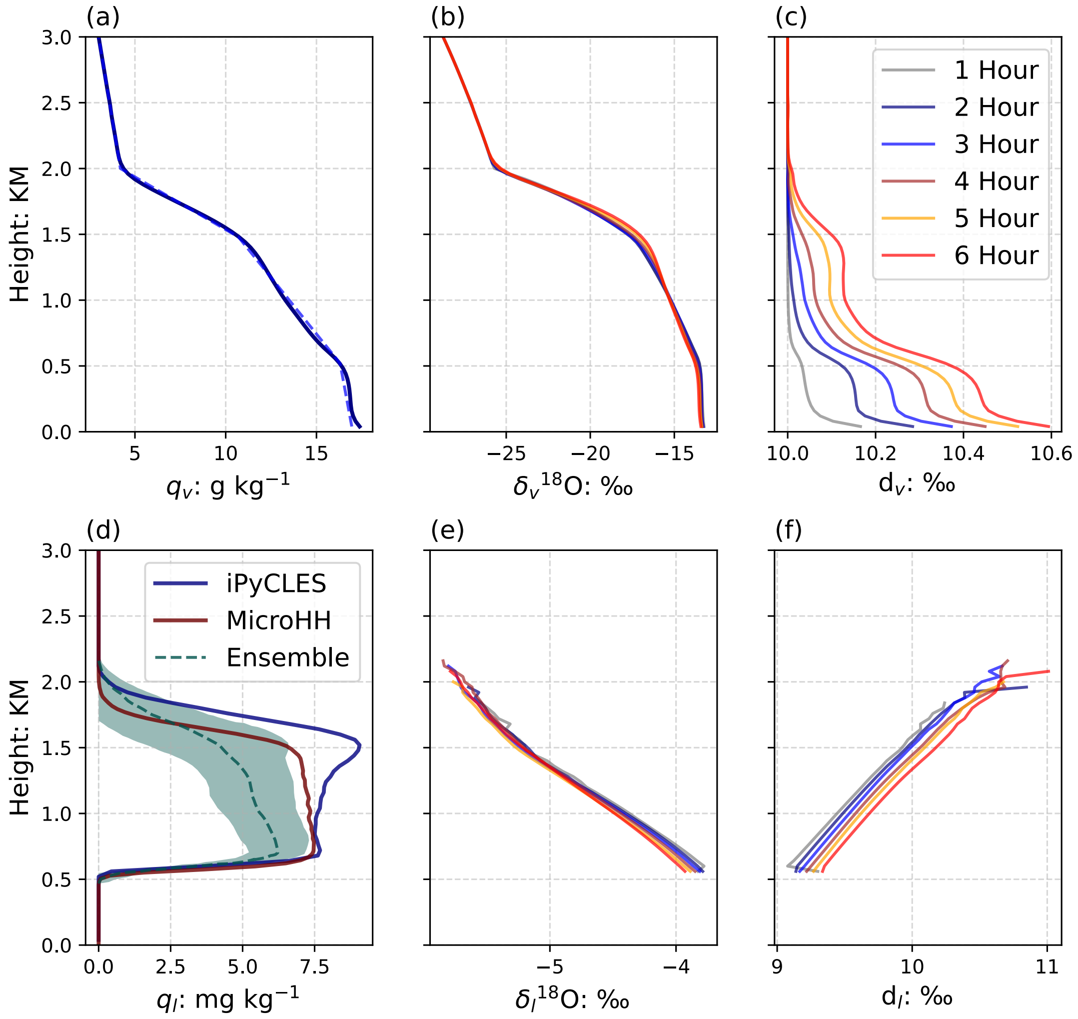

Vertical profiles of (a) domain-mean water vapor specific humidity over the last hour of the simulation and hourly-averaged (b) δ^{18}O and (c) deuterium excess (d) in water vapor; (d) domain-mean specific cloud liquid water content over the last hour of the simulation and hourly-averaged (b) δ^{18}O and (c) deuterium excess (d) in cloud liquid water from the BOMEX simulation. The dashed green line and shaded area in (c) show the LES ensemble mean and spread for the same case from Siebesma et al. (2003), and the dark red line in (c) shows a corresponding MicroHH simulation result (Bastak Duran et al., 2021).

Supplementary Material： iPyCLES in RICO case

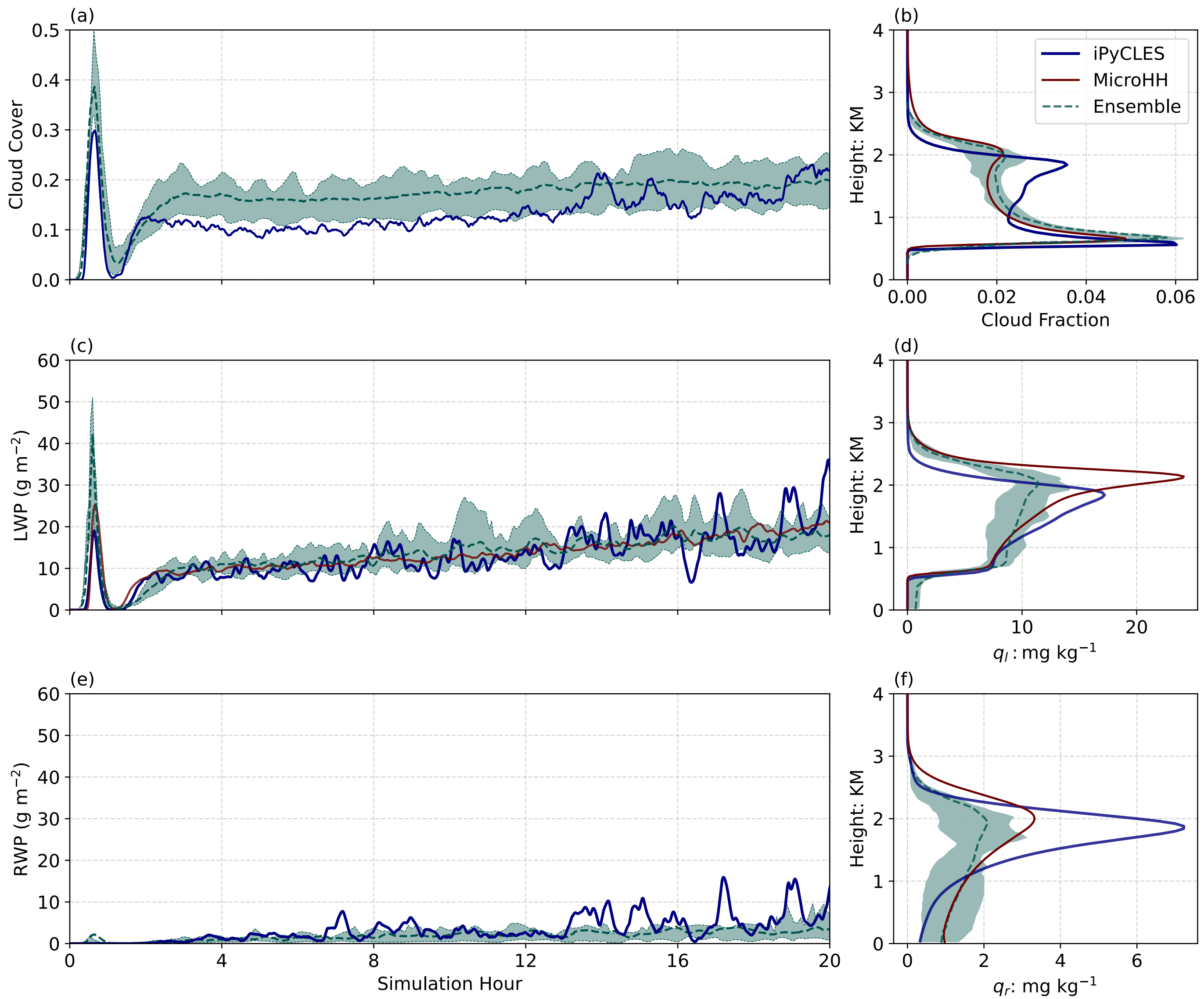

Time series of (a) cloud cover and vertically-integrated (c) liquid water path (LWP) and (e) rain water path (RWP) during the RICO case based on iPyCLES (dark blue). The right panels show vertical profiles of horizontal domain-averaged (b) cloud fraction, (d) specific cloud liquid water content ql, and (f) specific rain water content qr averaged over the last four hours of the simulation. The green dashed line and shading in each panel indicate the multi-model ensemble mean and spread from an earlier RICO intercomparison (van Zanten et al., 2011), while the dark red line shows a corresponding MicroHH simulation result (Bastak Duran et al., 2021).

Supplementary Material：iPyCLES in RICO case

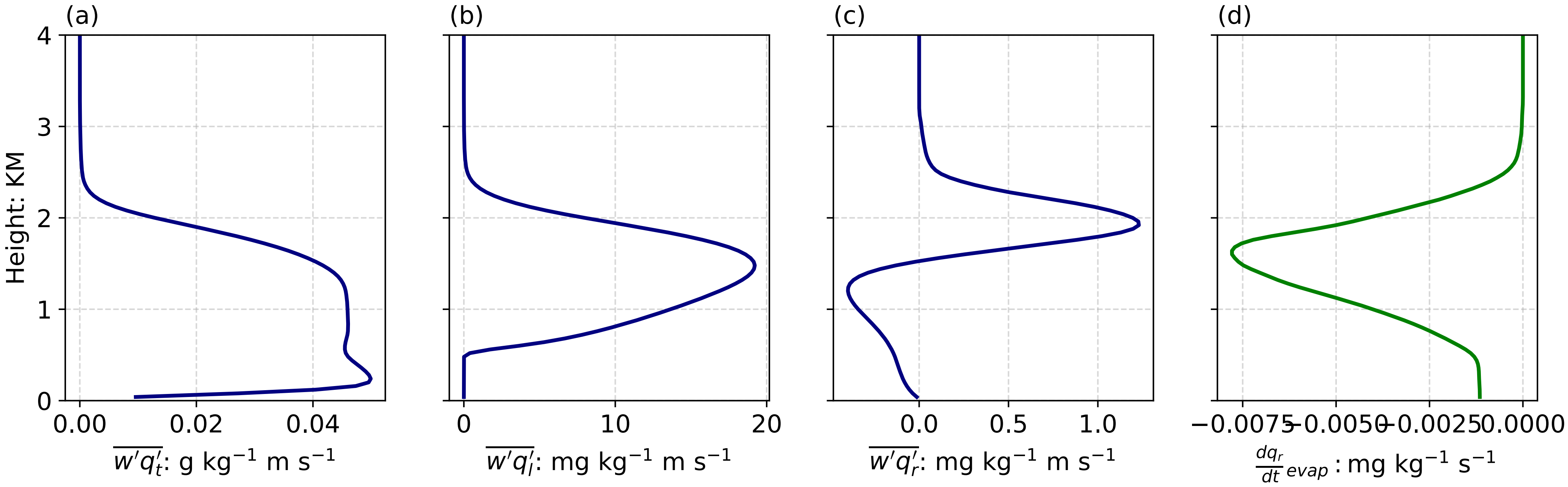

Domain-mean vertical turbulent fluxes from the RICO case for (a) total specific water content qt, (b) specific cloud liquid water content ql, and (c) specific rain water content qr, along with (d) the evaporation tendency for specific rain water content: $\frac{dq_r}{dt}$(evp) . All profiles are averaged from hour 4 to hour 20 of the simulation.

Supplementary Material: iPyCLES in RICO case

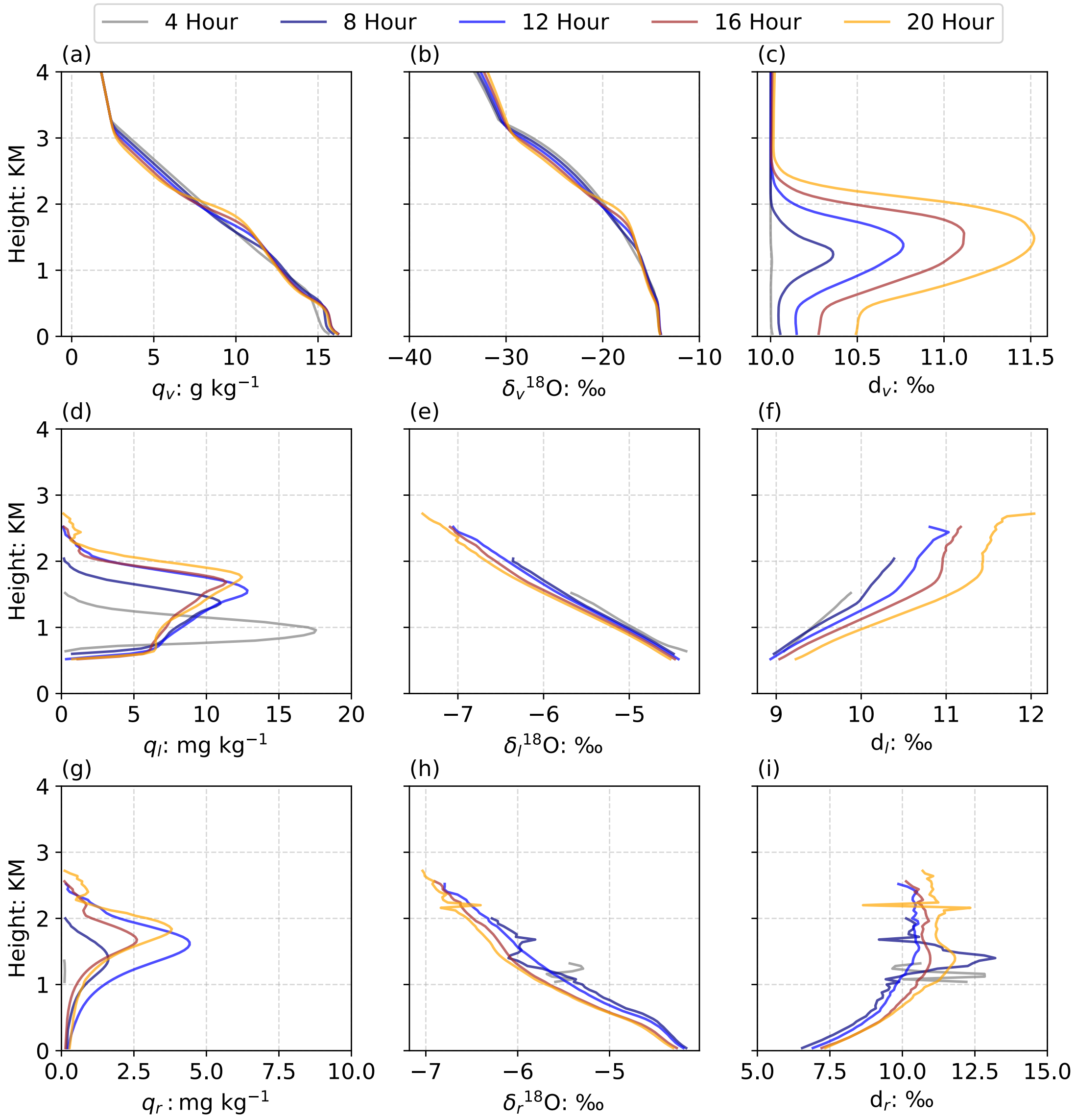

Vertical profiles of hourly-averaged (a) water vapor specific humidity, (b) δ^{18}O in water vapor, and (c) deuterium excess d in water vapor. Corresponding hourly-averaged specific water contents and isotopic compositions are also shown for (d-f) cloud liquid water and (g-i) rain. Profiles are averaged over the hour prior to the simulation time marked in the legend.

Supplementary Material： iPyCLES in ISDAC case

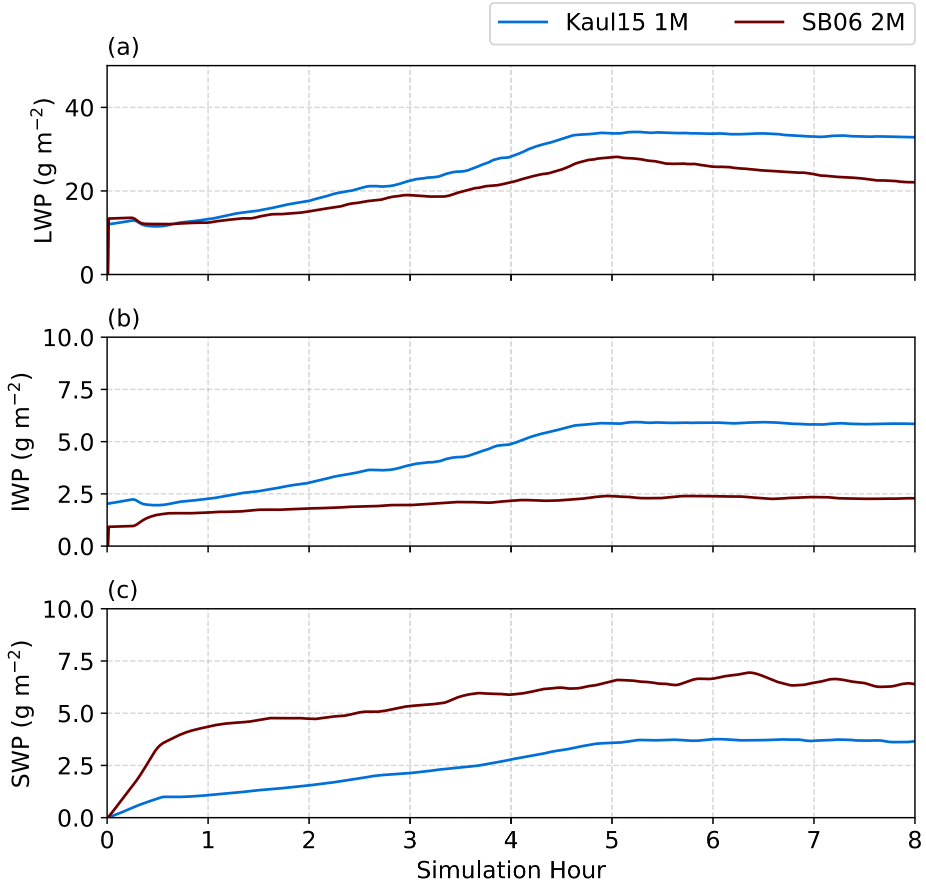

Time series of (a) cloud liquid water path (LWP), (b) cloud ice water path (IWP), and (c) snow water path (SWP) from the 8-hour ISDAC run. Results using both the Kaul15 one-moment (blue) and SB06 two-moment (red) microphysics are presented for comparison.

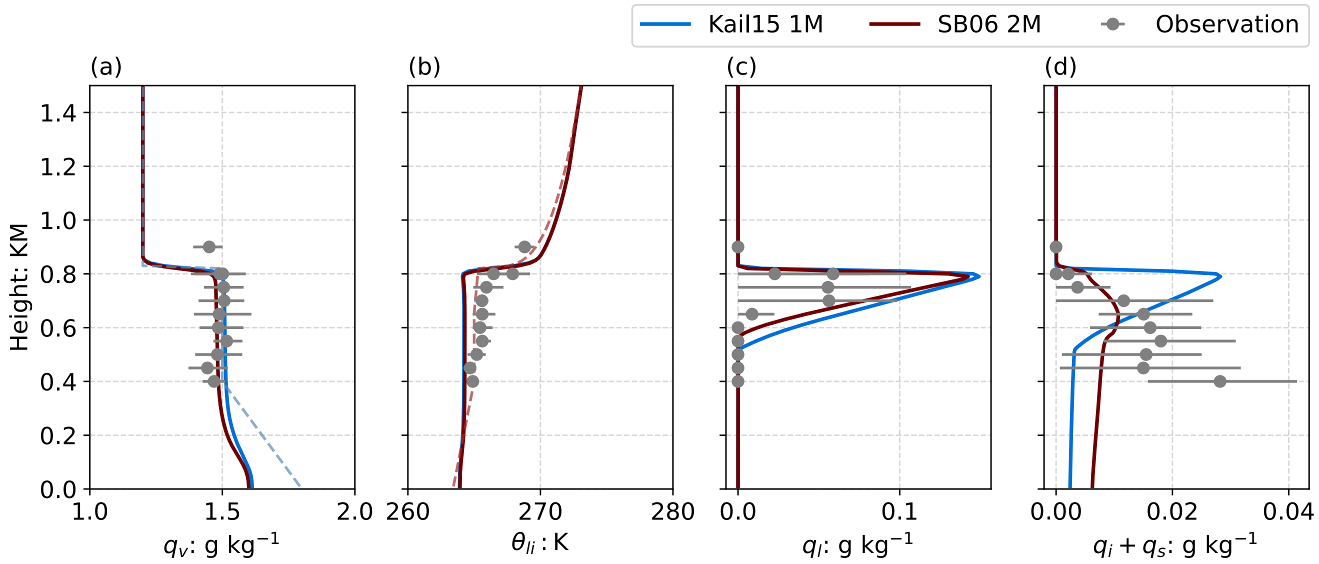

Vertical profiles of horizontal domain-mean (a) total specific water content qt, (b)liquid and ice potential temperature θli, (c) specific cloud liquid water content ql, and (d) total specific water content of cloud ice and snow qi + qs from the simulations using the Kaul15 (blue) and SB06 (red) mixed-phase microphysics. All profiles are averaged over hours 1–8 of the simulation. The initial conditions are shown as dashed lines in (a) and (b) for context. The grey dots show field measurements collected during flight 31 of ISDAC campaign on 27 April 2008, with uncertainty bars encompassing the 15–85% range of measurements collected at 50-m intervals from 400–900 m height (McFarquhar et al., 2011, their Fig. 14).

Supplementary Material： iPyCLES in ISDAC case

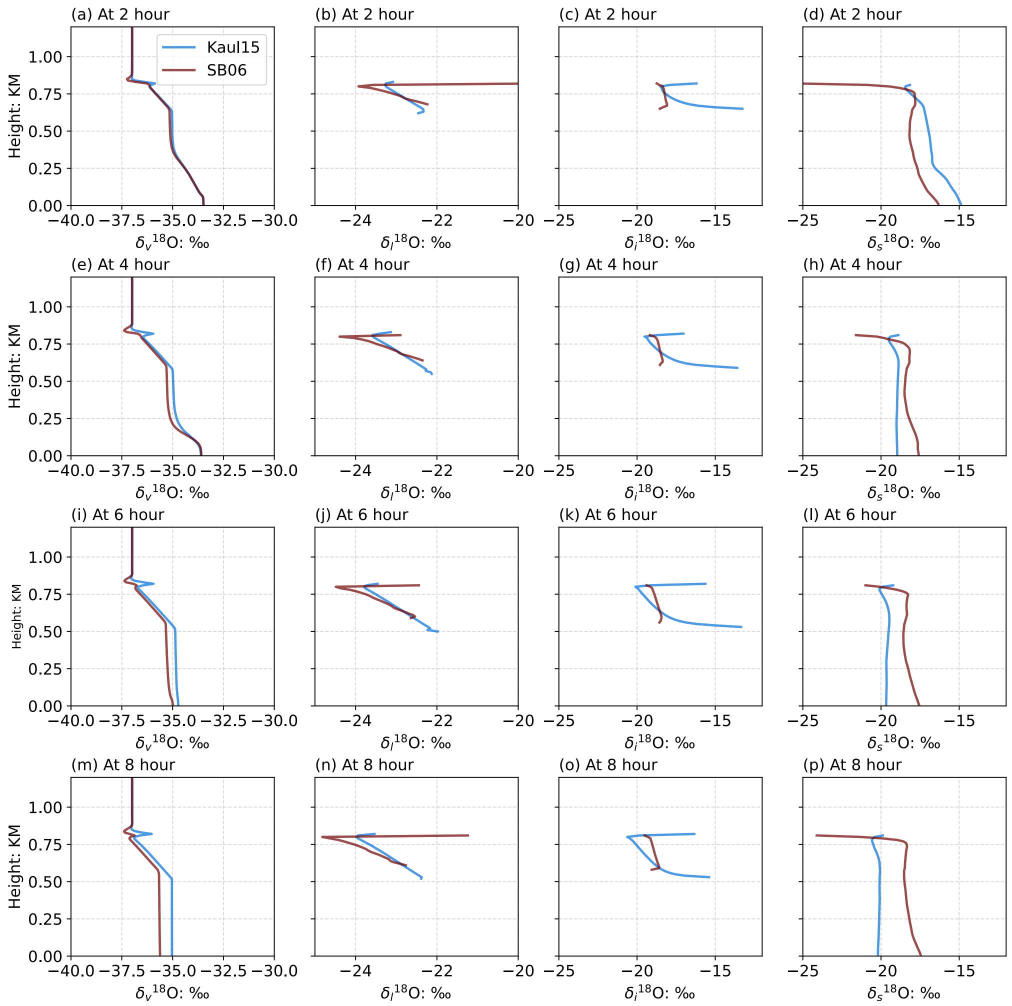

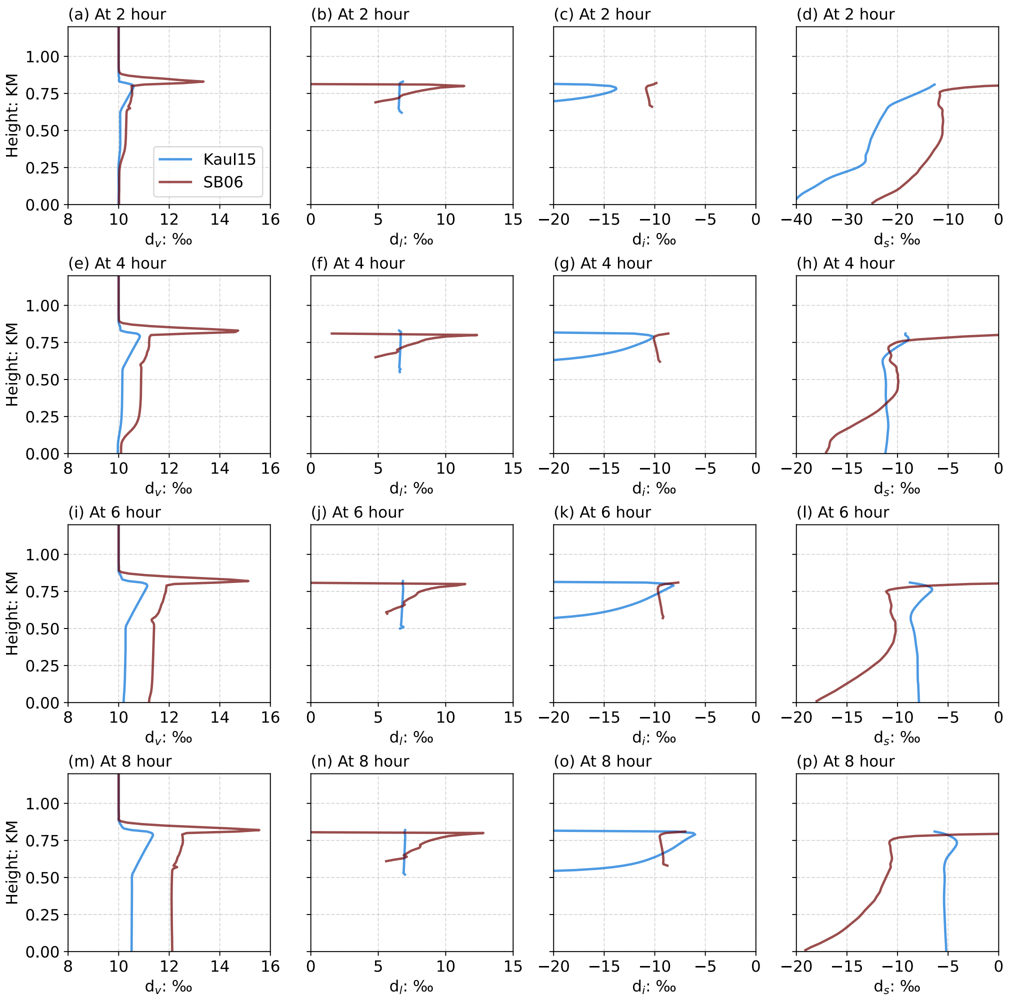

Horizontal domain-mean vertical profiles of δ^{18}O and d-excess in water vapor (first column), cloud liquid water (second column), cloud ice (third column), and snow (fourth column) simulated using iPyCLES with the Kaul15 microphysics (blue) and the SB06 microphysics (red). Profiles are 1-hour averages preceding hours 2, 4, 6, and 8 of each simulation.

Supplementary Material：iPyCLES in ISDAC case

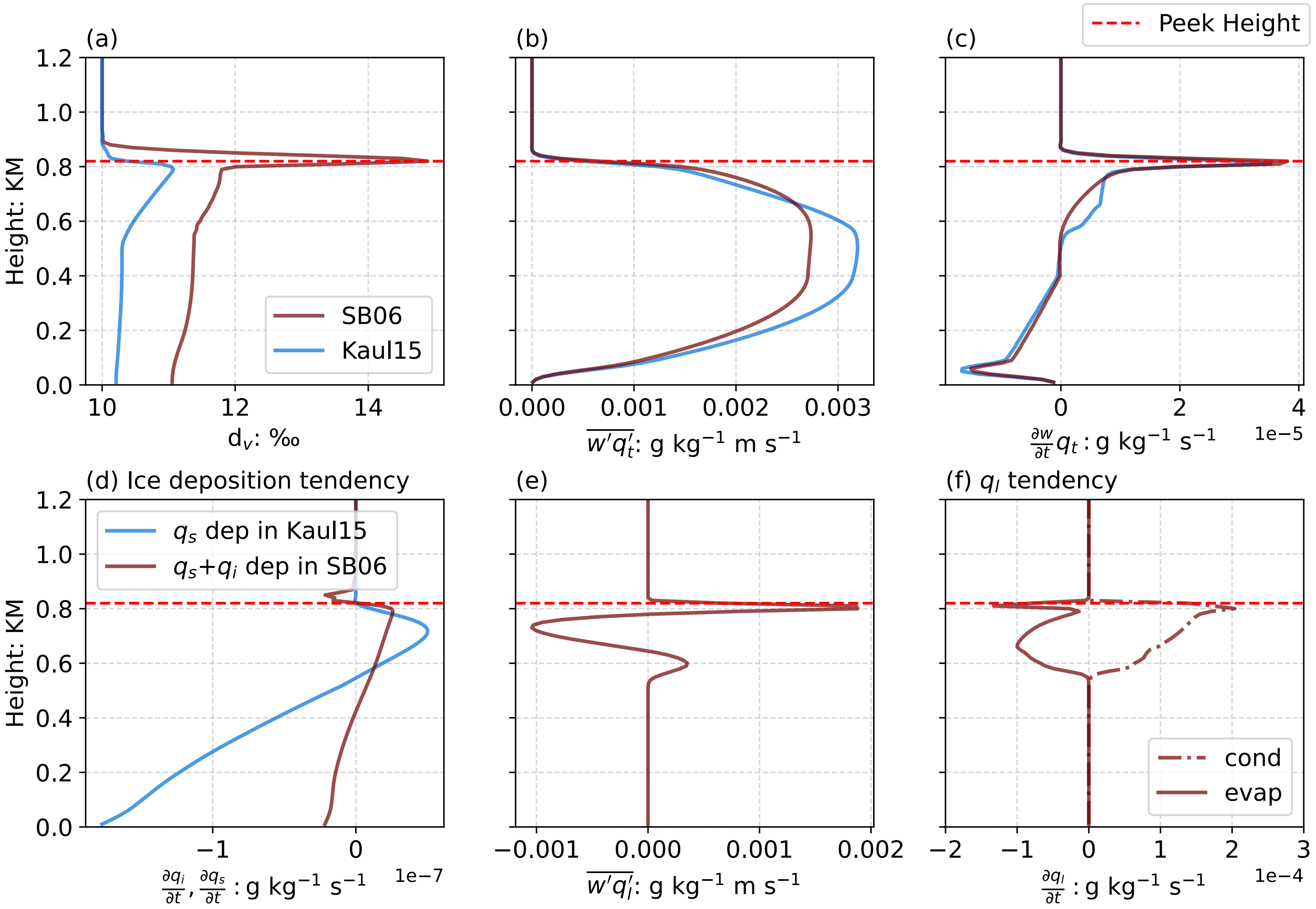

Vertical profiles of horizontal domain mean of diagnosed variables to explain the isotopic peek at cloud topic within SB06 scheme, with the compression from Kaul15 scheme: (a) profiles of deuterium excess of water vapor dv; (b) vertical flux of total specific water content qt; (c) vertical flux tendency of qt; (d) deposition and sublimation tendency of specific cloud ice water content qi; (e) vertical flux tendency of ql; (f) condensation(cond) and evaporation(evap) tendency of specific cloud liquid water content ql. The altitude of the isotopic peek is plotted by a dashed red line with 820 m height. The profiles from Kaul15 scheme are plotted in purple. Ice deposition/sublimation and cloud liquid evaporation/condensation in Kaul15 scheme are not included because of the diagnosed qi and ql within the mixed-phase saturation adjustment.

Supplementary Material： Experiment settings

Name	Surface Flux: W m^{-2}	Large-Scale Advection	θ inversion	q_t inversion	Forcing Isotope
BASE	Ice	None	Default	Default	Default
INVT	Ice	None	270 K	Default	Enriched
INTQ	Ice	None	270 K	1.6 g kg^{-1}	Enriched
SURF	SHF=20; LHF=24	None	Default	Default	Default
LSAD	Ice	dq_t/dt dT/dt	Default	Default	Enriched

Summary of simulation set-ups. The short name BASE is the control run, INVT refers to the simulation with the thermal inversion strength, INQT refers to the simulation with both thermal and moisture inversion strength, SURF indicates the sensible heat flux and latent heat flux at the surface adopted from reanalysis, and LSAD couples the large-scale advection source of temperate and water vapor acquired from reanalysis. The default value of θ inversion is 266 K, and qt inversion is 1.2 K..

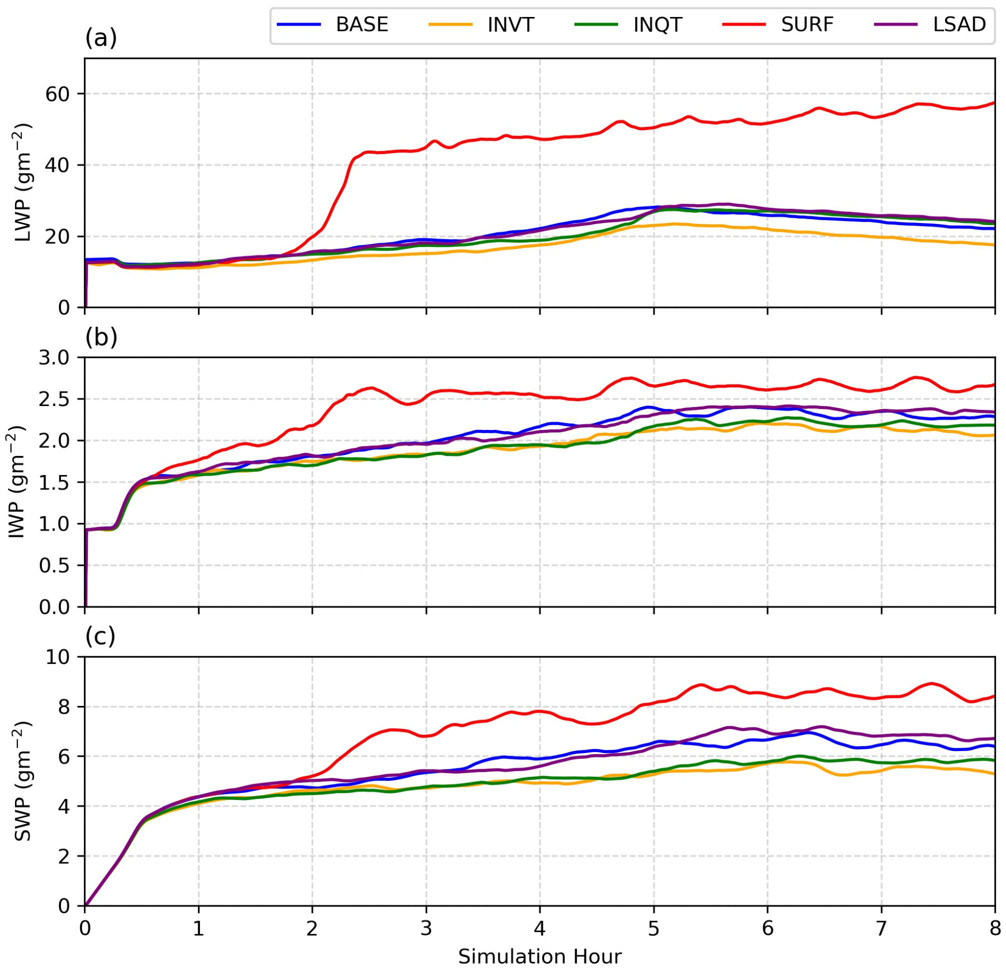

Time series of five different simulation results: (a) Liquid water path LWP; (b) Ice water path IWP; and (c) Snow water path.

Supplementary Material：INQT&INVT experiment performance

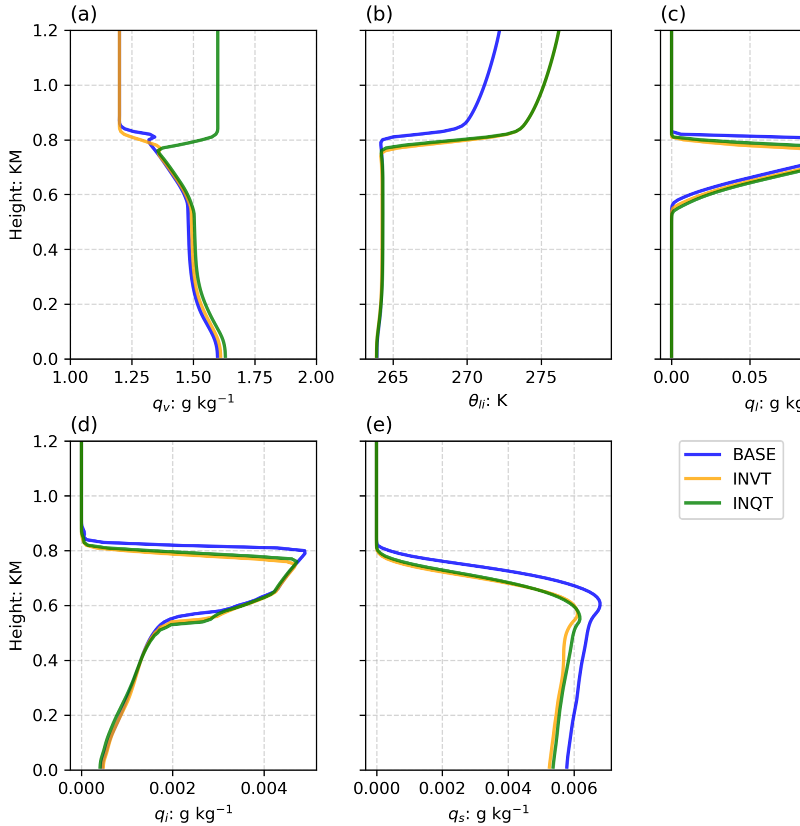

Vertical profiles of the horizontal domain average after first spin-up hour for simulation BASE, INVT and INQT, includes (a) vapor specific humidity qv, (b) liquid ice potential temperature θli, (c) cloud liquid specific humidity ql, (d) cloud ice specific humidity qi and (e) snow specific humidity qs.

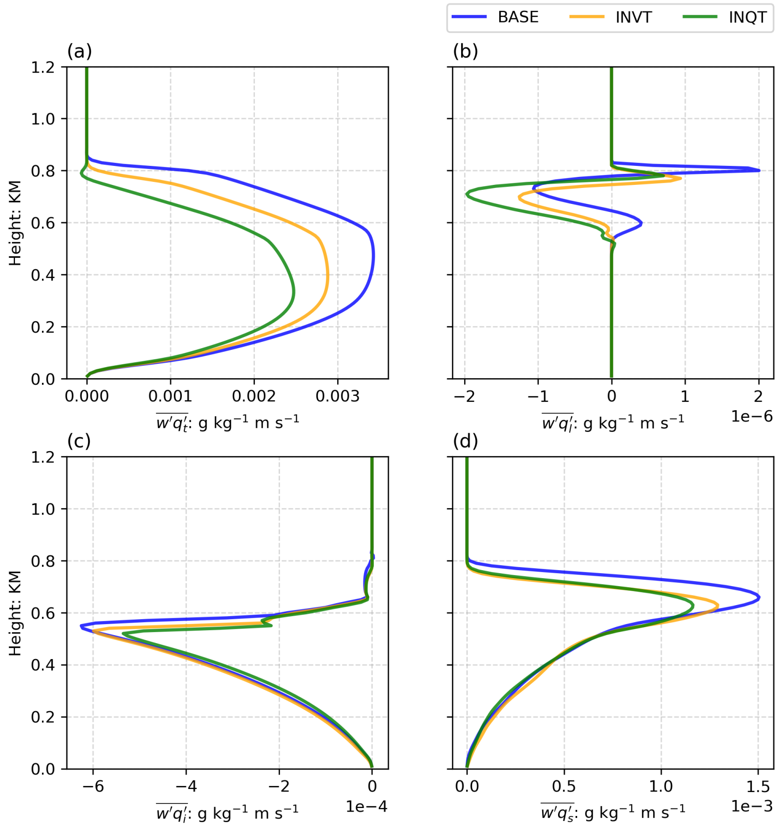

Profiles of resolved turbulent flux at the vertical direction. The horizontal domain averages after the first spin-up hour for simulation BASE, INVT and INQT, are shown for (a) total water specific humidity, (b) cloud liquid specific humidity, (c) cloud ice specific humidity; and (d) snow specific humidity.

Supplementary Material：INQT&INVT experiment performance

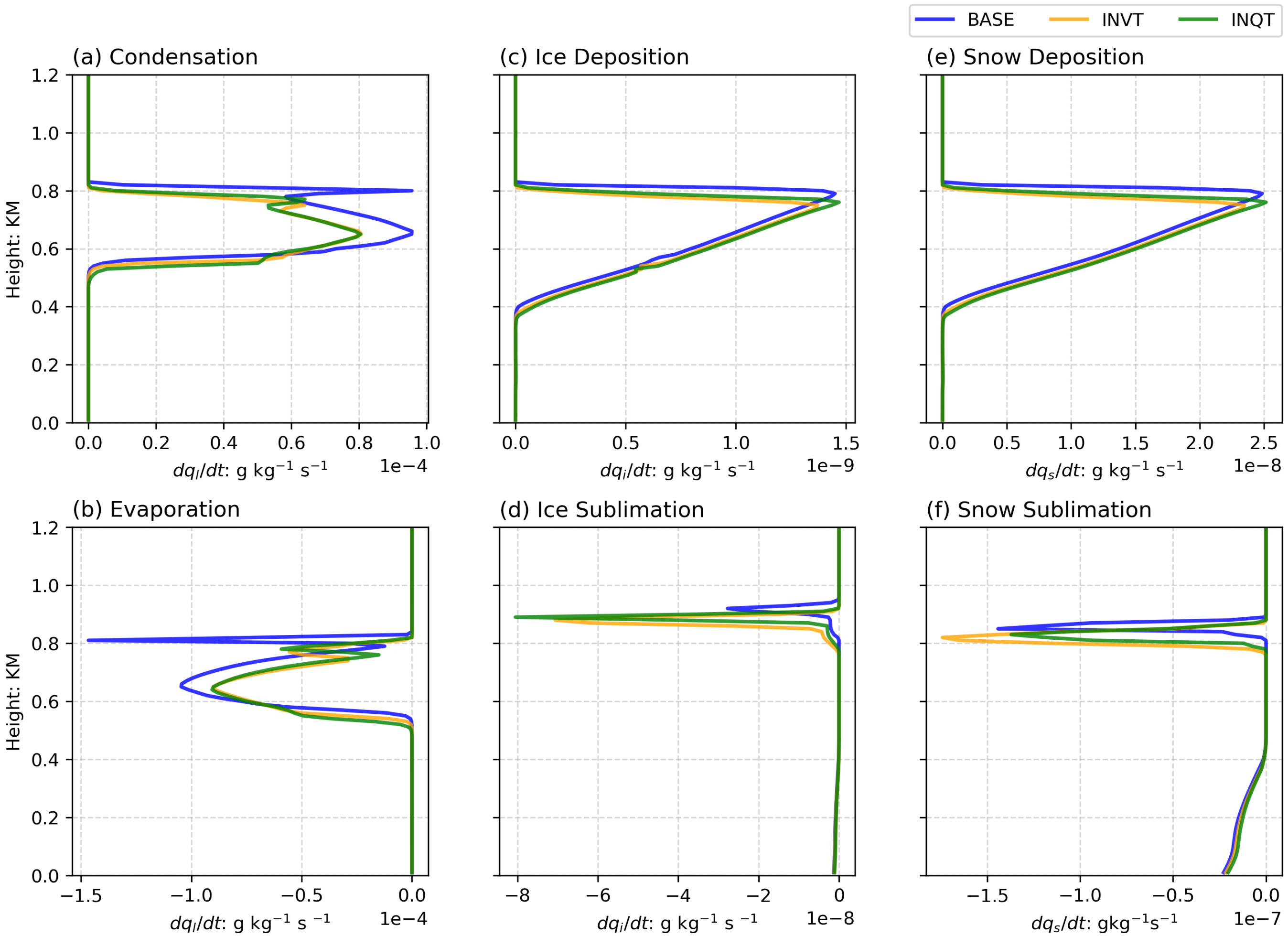

Vertical Profiles of microphysical tendencies of different species. The horizontal domain averages after the first spin-up hour for simulation BASE, INVT and INQT, are shown for (a) condensation of cloud droplets; (b) evaporation of cloud droplets; (c) deposition of ice crystal; (d) sublimation of ice crystal; (e) deposition of snow; and (f) sublimation of snow

Supplementary Material：INQT&INVT experiment performance

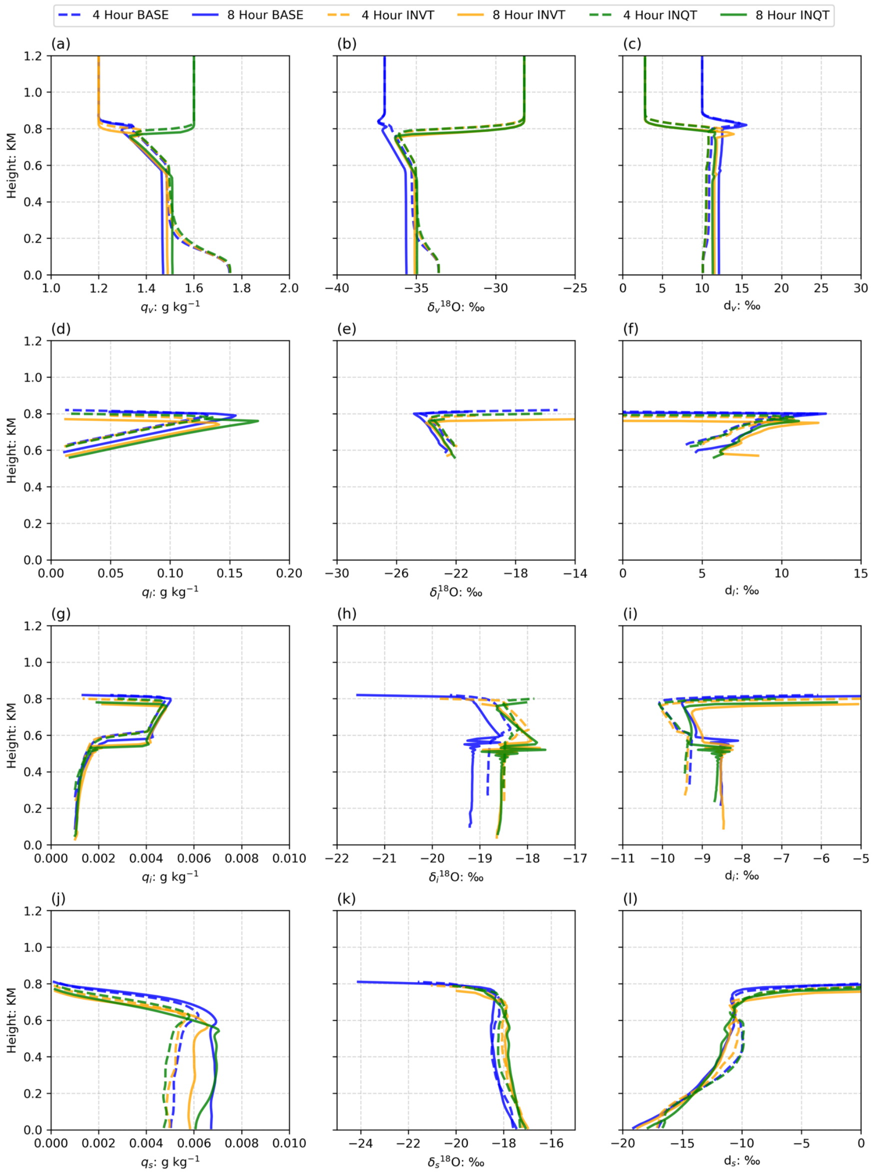

Vertical profiles of the horizontal domain mean for the vapor specific humidity and vapor isotopic composition (a-c), cloud liquid specific humidity and droplet isotope composition (d-f), cloud ice specific humidity and ice isotope composition (h-j), and snow specific humidity and isotope composition (j-l) in the simulation BASE, INVT and INQT. The 4th and 8th hour during the simulation are selected for comparison, which are shown as dashed and solid lines respectively. The isotopic composition of each species is evaluated by the isotope ratio δ and deuterium excess d.

Supplementary Material: SURF experiment performance

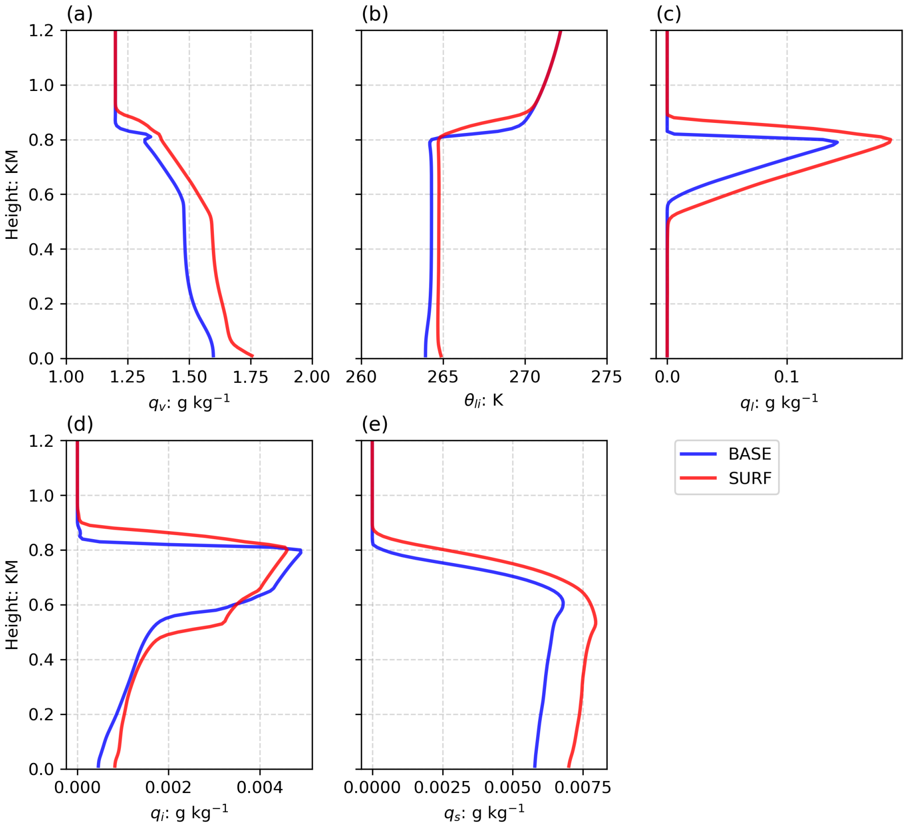

Vertical profiles of the horizontal domain average after first spin-up hour for simulation SURF and BASE, includes (a) vapor specific humidity qv, (b) liquid ice potential temperature θ_{li}, (c) cloud liquid specific humidity ql, (d) cloud ice specific humidity qi and (e) snow specific humidity qs.

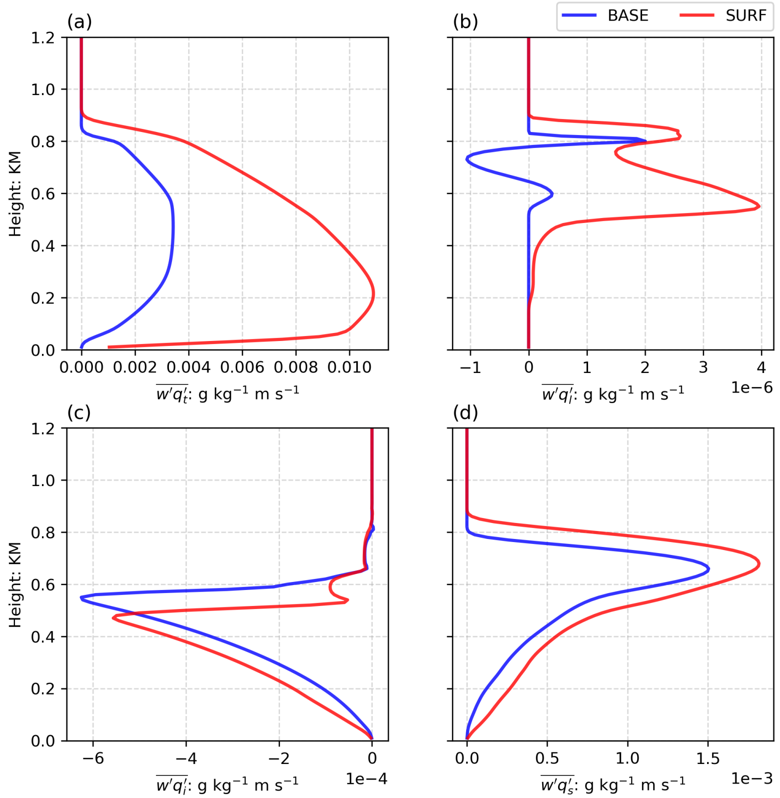

Profiles of resolved turbulent flux at the vertical direction. The horizontal domain averages after the first spin-up hour for simulation SURF and BASE, are shown for (a) total water specific humidity, (b) cloud liquid specific humidity, (c) cloud ice specific humidity; and (d) snow specific humidity.

Supplementary Material: SURF experiment performance

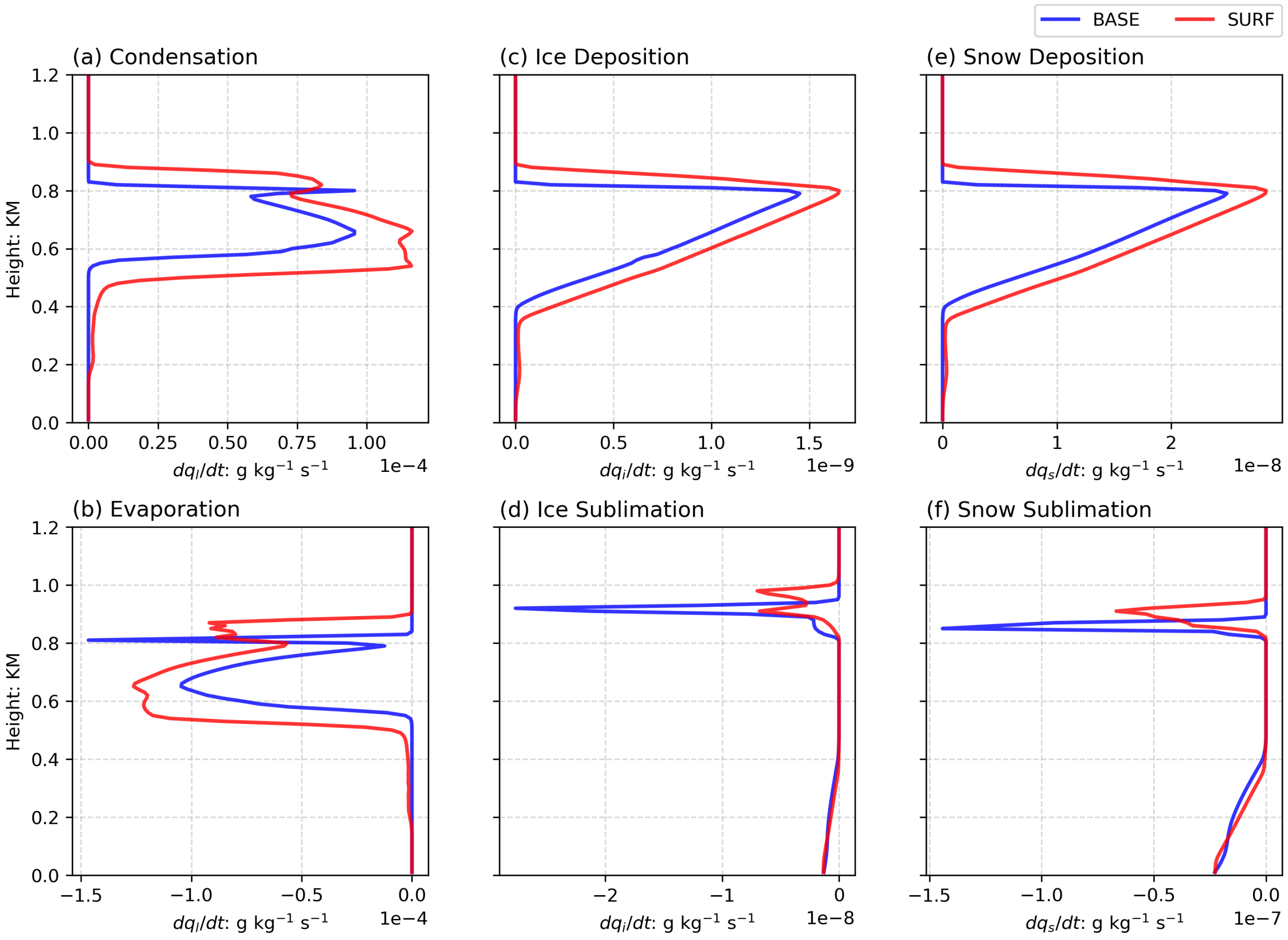

Vertical Profiles of microphysical tendencies of different species. The horizontal domain averages after the first spin-up hour for simulation BASE and SURF, are shown for (a) condensation of cloud droplets; (b) evaporation of cloud droplets; (c) deposition of ice crystal; (d) sublimation of ice crystal; (e) deposition of snow; and (f) sublimation of snow

Supplementary Material： SURF experiment performance

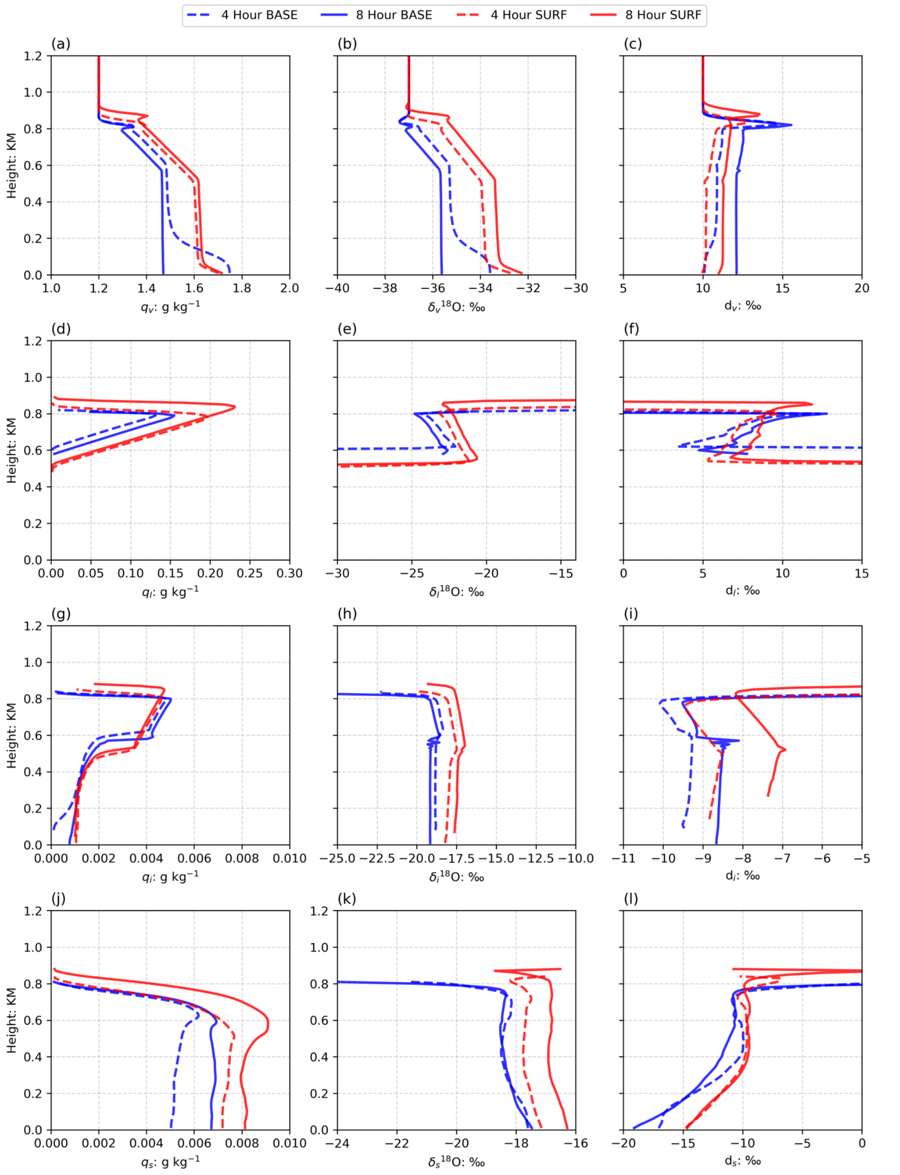

Vertical profiles of the horizontal domain mean for the vapor specific humidity and vapor isotopic composition (a-c), cloud liquid specific humidity and droplet isotope composition (d-f), cloud ice specific humidity and ice isotope composition (h-j), and snow specific humidity and isotope composition (j-l) in the simulation BASE and SURF. The 4th and 8th hour during the simulation are selected for comparison, which are shown as dashed and solid lines respectively. The isotopic composition of each species is evaluated by the isotope ratio δ and deuterium excess d.

Supplementary Material: LSAD experiment performance

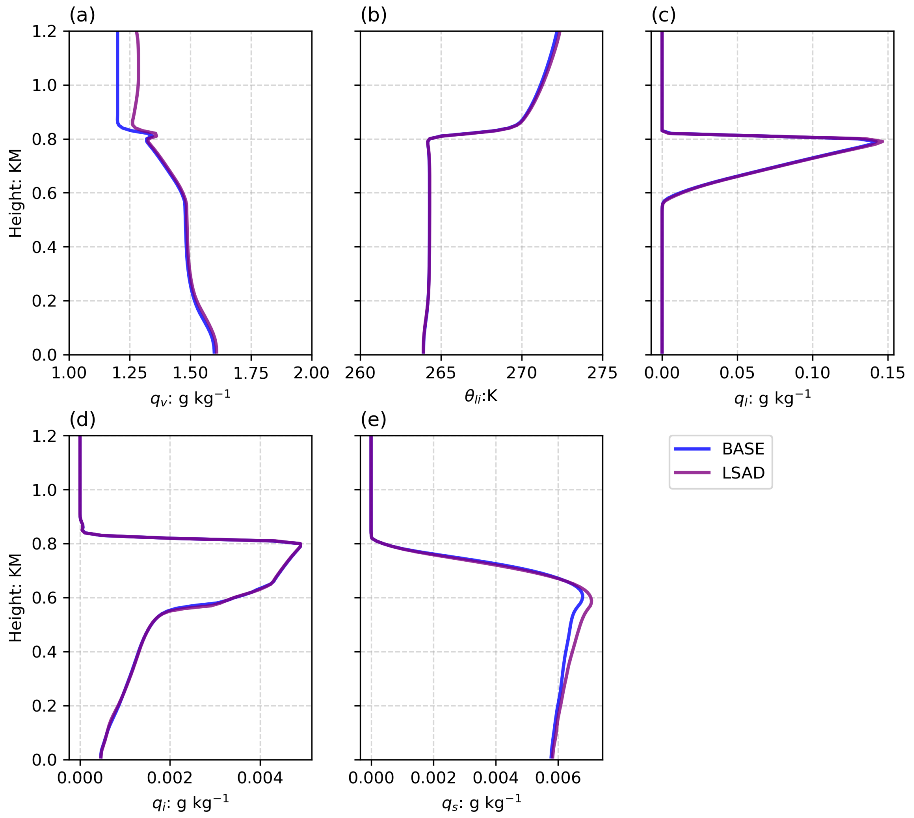

Vertical profiles of the horizontal domain average after first spin-up hour for simulation LSAD and BASE, includes (a) vapor specific humidity qv, (b) liquid ice potential temperature θ_{li}, (c) cloud liquid specific humidity ql, (d) cloud ice specific humidity qi and (e) snow specific humidity qs.

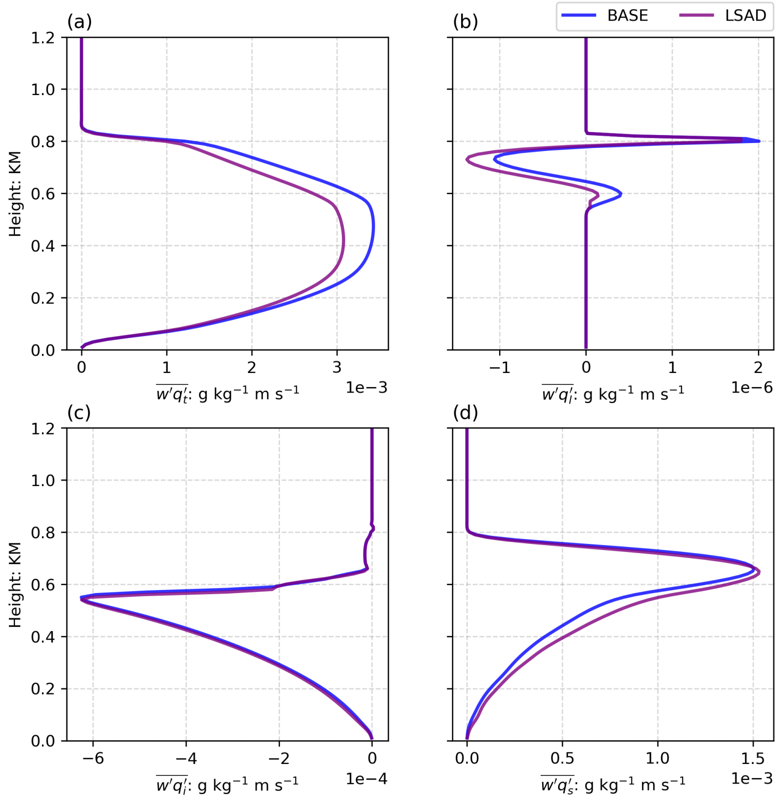

Profiles of resolved turbulent flux at the vertical direction. The horizontal domain averages after the first spin-up hour for simulation LSAD and BASE, are shown for (a) total water specific humidity, (b) cloud liquid specific humidity, (c) cloud ice specific humidity; and (d) snow specific humidity.

Supplementary Material: LSAD experiment performance

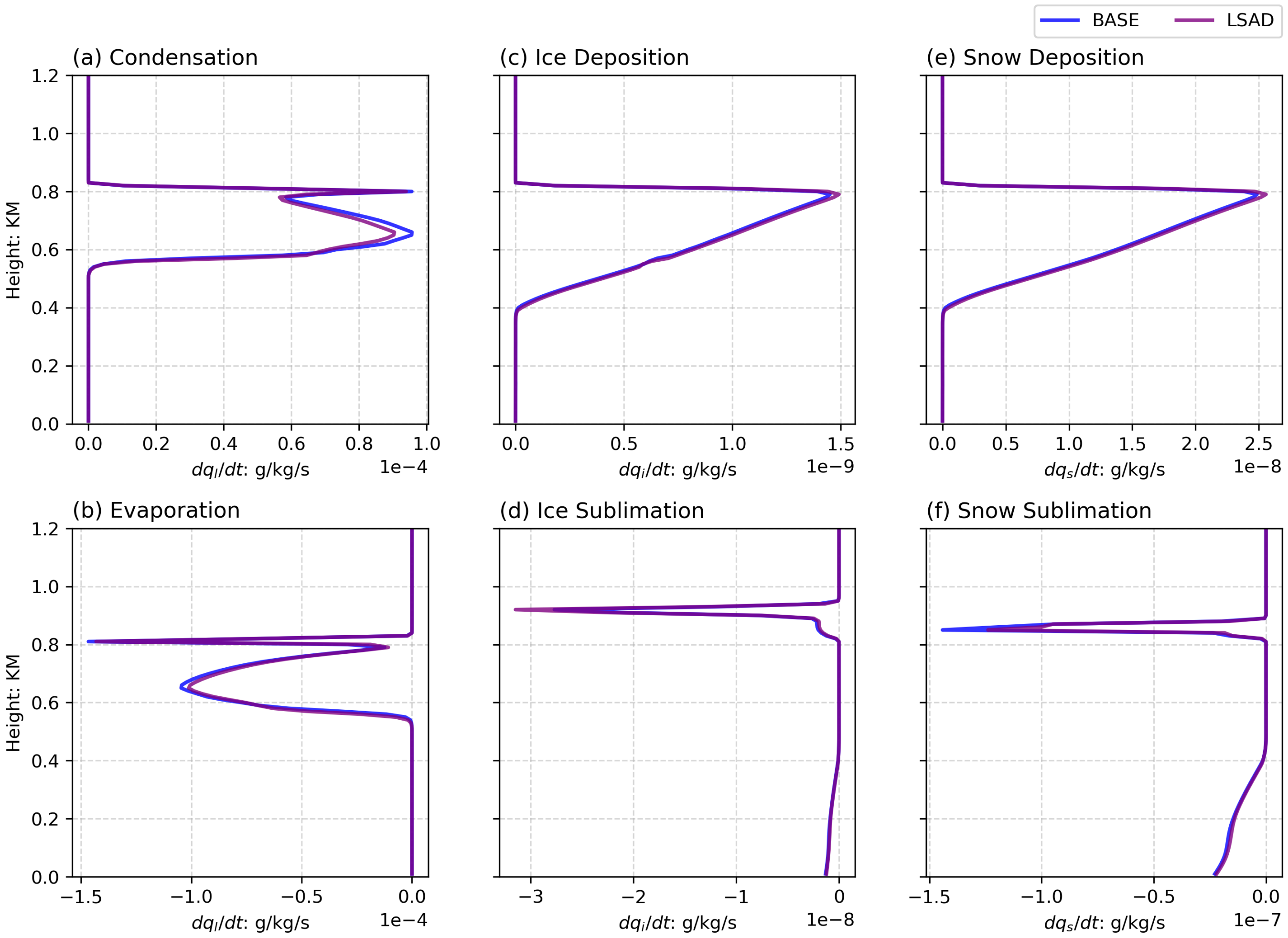

Vertical Profiles of microphysical tendencies of different species. The horizontal domain averages after the first spin-up hour for simulation BASE and LSAD, are shown for (a) condensation of cloud droplets; (b) evaporation of cloud droplets; (c) deposition of ice crystal; (d) sublimation of ice crystal; (e) deposition of snow; and (f) sublimation of snow

Supplementary Material: LSAD experiment performance

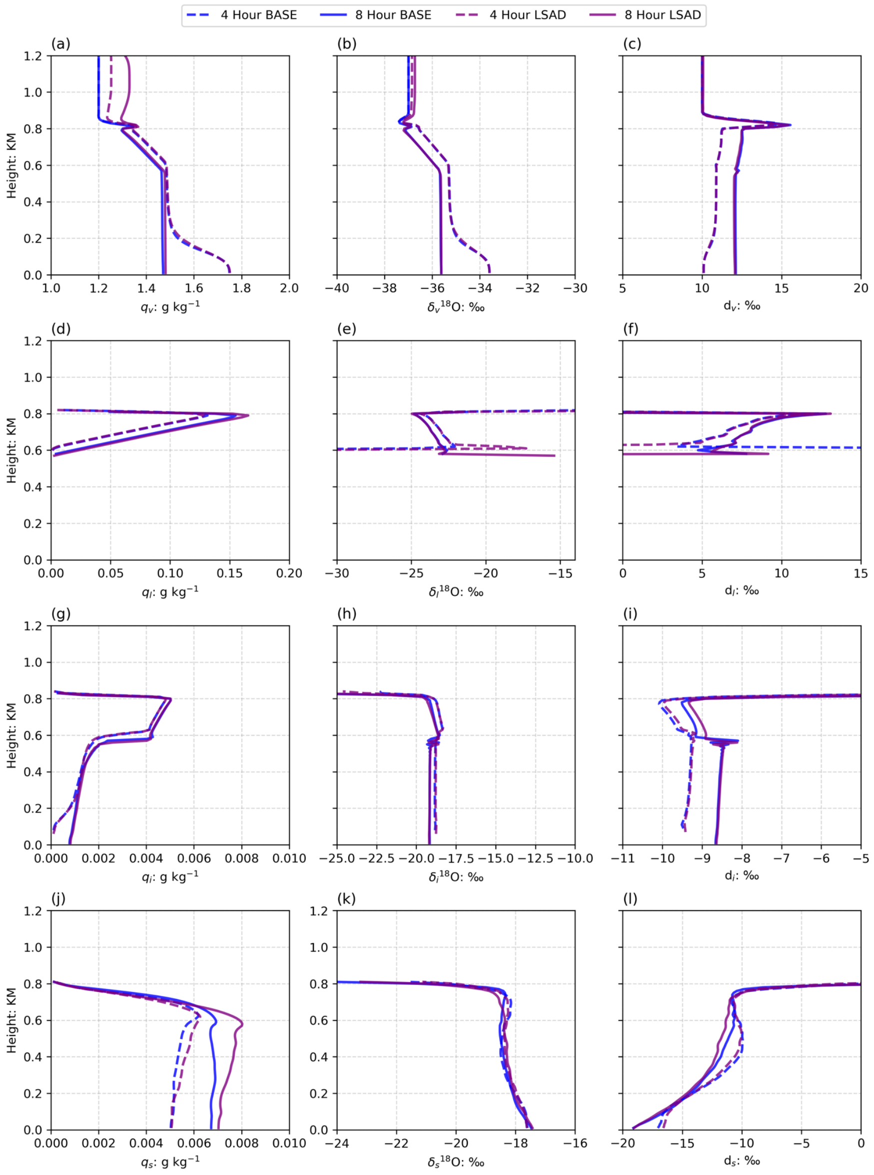

Vertical profiles of the horizontal domain mean for the vapor specific humidity and vapor isotopic composition (a-c), cloud liquid specific humidity and droplet isotope composition (d-f), cloud ice specific humidity and ice isotope composition (h-j), and snow specific humidity and isotope composition (j-l) in the simulation BASE and LSAD. The 4th and 8th hour during the simulation are selected for comparison, which are shown as dashed and solid lines respectively. The isotopic composition of each species is evaluated by the isotope ratio δ and deuterium excess d.